Check for updates

Proceedings of the 2024 Design of Medical Devices Conference
DMD2024
April 8-10, 2024, Minneapolis, MN, USA

DMD2024-1076

Downloaded from http://asmedigitalcollection.asme.org/BIOMED/proceedings-pdf/DMD2024/87752/V001T02A009/7379084/v001t02a009-dmd2024-1076.pdf by guest on 28 January 2025

MIGRATION OF LEUKOCYTES IN SHEAR FLOWS: INSIGHTS FROM SIMULATIONS

Tam T. Nguyen
Department of Civil, Construction, and Environmental Engineering
North Dakota State University
Fargo, ND
USA

Lahcen Akerkouch
Department of Civil, Construction, and Environmental Engineering
North Dakota State University
Fargo, ND
USA

Trung B. Le
Department of Civil, Construction, and Environmental Engineering
North Dakota State University
Fargo, ND
USA

ABSTRACT

The objective of this study is to investigate the rolling dynamics of leukocytes in microchannel flows using a hybrid continuum-particle approach. Leukocytes play an essential role in the immune system, and their margination behavior has been extensively studied both experimentally and numerically. In this study, we have developed a series of numerical experiments using a hybrid DPD-CFD solver with the membrane stiffness of the modeled leukocytes as the primary investigation subject. Our results show that increasing the stiffness of the cell's membrane influences its deformability and trajectory in microchannel flows. The results obtained from this study could be valuable in designing next-generation micro-carriers for targeted drug delivery systems, which mimic the margination behavior of leukocytes.

Keywords: Continuum-Particle Method, White Blood Cells, Cell-Fluid Interaction, Margination.

NOMENCLATURE

CFL	Computational Fluid Dynamics
DPD	Dissipative Particle Dynamics
FSI	Fluid-Solid Interaction
GMRES	Generalized Minimal Residual
RBC	Red Blood Cell
WBC	White Blood Cell

1. INTRODUCTION

The circulatory system, a vital network of organs encompassing the heart, blood vessels, and blood, serves as the body's transportation system. Comprising the heart, arteries, veins, and blood, it orchestrates a synchronized effort to circulate oxygen, nutrients, hormones, and waste products throughout the body. The heart propels blood through arteries, while veins return it, completing a continuous cycle. This intricate system ensures the delivery of essential elements and the removal of metabolic byproducts, playing a pivotal role in sustaining life and maintaining physiological balance.

Within the circulatory system, Erythrocytes (RBCs) carry out the most critical functions of the blood in the circulatory system, which is cycling substances around the body. On the other hand, Leukocytes (WBCs) play a crucial role in the body's immune system by identifying and neutralizing pathogens, such as bacteria and viruses. The main driver for cell migration through the circulatory system is a low-Reynolds number, pressure-driven flow caused by the heart. The variety in size of capillaries has a significant impact on the Reynolds number, which can range from 1.7E-3 when the diameter is 5 micrometers to 0.7 if the diameter is 100 micrometers [1]. The Fåhræus–Lindqvist effect is a significant phenomenon in blood vessels with a diameter of less than 300 micrometers. It describes an increase of the apparent viscosity with increasing tube diameter. The hydrodynamic effects lead to the formation of two phases for cross-stream migration of blood components: a flow core consisting mainly of RBCs and a Cell-Free Layer (CFL) [2]. Since WBCs' membrane is more rigid than RBSs, they migrate toward the blood vessel wall via margination. Some suggested that the margination of white blood cells (WBCs) towards vessel walls is an essential precondition for their arrest and rolling phases on the vascular endothelium [3].

The margination of WBCs is a complex phenomenon that has been extensively studied, both experimentally and numerically. Various factors, including shear rate, vessel diameter, flow conditions, and hematocrit values influence the phenomenon [4]. While the mechanism remains unknown, the phenomenon has inspired a new generation of micro-carriers for targeted drug delivery. Developing carriers that mimic this margination

© 2024 by ASME

behavior could address the difficulty in achieving high efficiency and precision of maneuverability and stability [5].

In this context, identifying key players in WBC's margination could be valuable in designing and advancing the development of next-generation micro-carriers. Developing a deeper understanding of phenomena, such as the margination of WBCs, could open up new avenues for targeted drug delivery systems and further advance the field of biomedical engineering. Motivated by this, we have developed a series of numerical experiments using a hybrid DPD-CFD solver with the membrane stiffness of the modeled WBCs as the main investigation subject. The results from our experiments show that increasing stiffness of the cell's membrane influences its deformability and trajectory in microchannel flows.

2. MATERIALS AND METHODS

2.1 Cell Modeling Method

Our approach to modeling biological cells involves the use of the Dissipative Particle Dynamics (DPD) method. DPD groups atoms and particles into an entity through a process called coarse-grained representation, which is particularly suitable for modeling complex systems like biological cells. By allowing the simulation of higher spatial and temporal scales, DPD can be coupled with a similar coarse-grain method or a continuum solver in our approach.

TABLE 1. GEOMETRICAL PARAMETERS OF WBC'S MEMBRANE.

Cell Diameter	Surface Area	Volume
D_0 (μm)	A_0 (μm^2)	V_0 (μm^3)
7.0	153.8	179.6

TABLE 2. MODEL PARAMETERS FOR WBC USED IN THE SIMULATIONS.

Shear Modulus	Persistence Length	Maximum Extension Length
μ_0 ($pN/\mu m$)	p (μm)	l_m (μm)
4.7E+3	1.8E-3	0.59

Bending Stiffness	Force Coefficient
k_p (Nm^2)	k_c (J)
1.5E-24	2.4E-18

2.2 DPD Parameters for WBC Stretching Tests

We have used the DPD method to model two components of white blood cells (WBCs): the membrane and the plasma. For the membrane, we have generated a network of particles using an equation for a sphere. The cell diameter and extra geometrical parameters are listed in Table 1.

TABLE 3. LEUKOCYTE CONFIGURATIONS USED IN THE STRETCH TESTS.

Cytoplasm configurations:		
# particles		65
Membrane configurations:		
Case No.	# particles	# elements
1	246	488
2	498	992
3	1062	2120
4	2070	4136
5	4098	8192

In comparison to the cell's cytoplasm, parameters for DPD models of the membrane are extracted carefully and compared to different sources in the literature. Calibration of DPD models is always a crucial step before any production simulations to ensure the reliability of the models as DPD is an empirical method. Table 2 lists the parameters we have used in our model.

The interacting forces between the particles are the sum of in-plane elastic energy, bending, area, and volume potentials. In a similar implementation of the DPD method for the case of RBCs, it has been reported [6] that the membrane requires at least 500 DPD particles to behave accurately in the stretch test. In our study, we performed a stretch test mimicking a pair of microbeads pulling the WBCs in opposite directions with a total force of 15 micro-Newton. Table 3 lists five cases in the sensitivity analysis test where the membrane configurations differ.

2.3 Flow Solver and Coupling Method

We use the three-dimensional, unsteady incompressible continuity and Navier-Stokes equations to govern the external plasma. To couple the CFD and DPD methods, we employ a two-way coupling approach with the curvilinear immersed boundary (CURVIB) method [7]. The discrete equations are integrated over time using a fractional step method. For solving the momentum equations, we use a Newton-Krylov solver in the momentum step, and a GMRES solver with a multigrid pre-conditioner is used for the Poisson equation.

2.4 FSI Simulation Setup

In numerical experiments to study the influence of membrane stiffness on the rolling dynamics of leukocytes, we used Pointwise software to generate a rectangular microchannel whose width and height are 5 times the cell diameter, while the length is 20 times. The WBCs have a fixed number of particles for both the cytoplasm and the membrane which are 65 and 660, respectively.

Figure 1 shows the location of the cell which is at the center of the crosswise plane of the blood plasma grid while being at a distance of 5 times the cell diameter from the left wall to minimize the impact of prescribed conditions at the inlet. The total number of grid points is 3 million. Uniform velocity is

Downloaded from http://asmedigitalcollection.asme.org/BIOMED/proceedings-pdf/DMD2024/87752/V001T02A009/7379084/v001t02a009-dmd2024-1076.pdf by guest on 28 January 2025

 © 2024 by ASME

prescribed at the inlet while a fully developed profile is prescribed at the outlet. No-slip wall is prescribed for other faces to complete the boundary conditions. We fixed the WBCs in place and disabled two-way coupling (FSI) for the first 1000 time steps. During this time, the CFD solver would reach a steady-state solution, and an equilibrium state should be reached for the cells. Only then, the FSI module was enabled.

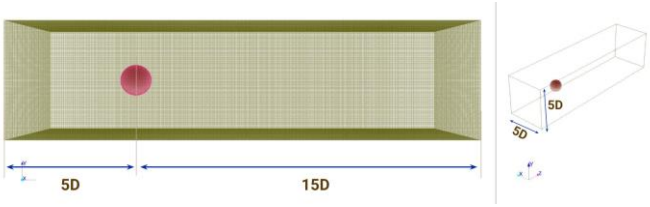

FIGURE 1. *SIMULATION SETUP SHOWING A 3D UNIFORM STRUCTURED GRID FOR THE BLOOD PLASMA (IN GOLD). WHILE THE WBC IS PRESENTED BY A TRIANGULATED MESH (IN MAGENTA).*

3. RESULTS AND DISCUSSION

3.1 Evolution of Axial and Transverse Diameters versus External Force

Throughout the stretch tests, we meticulously recorded the axial (left-to-right) and transverse (top-to-bottom) diameters after each load-application step. Figure 2's curves show less variation than those obtained from the RBC stretch test [6]. Despite the initial spherical shape, the axial displacement had a greater magnitude (4 micrometers) in comparison to the transverse displacement (1 micrometer). This discrepancy could be attributed to the underestimation of transverse diameter evolution by the DPD method [6].

However, all curves remain bounded, indicating that circulating cells with stiff membranes, such as leukocytes, necessitate a smaller number of DPD particles.

3.2 Rolling-Induced Dynamics by Membrane Stiffness in FSI Simulations

Figures 3 and 4 show the continuum mesh adaptively changed according to the movement of the cell. As the result of the CURVIB method, the Navier-Stokes solver only solved for flow solutions in the volume without the occupy of the cell's volume. A trace of the WBC (region with zero velocity submerged within the flow field) can be tracked in many cut planes without visualizing the DPD particles. Our method allows the hemodynamics outside the cell to be captured in high fidelity.

By tracking the top and bottom DPD points and plotting them in tandem with the cell's displacement, Figure 4 clearly shows that the WBC was rolling when migrating downstream. The traces of immersed nodes on vertical and horizontal middle-cut planes further tell the direction of the movement, which is upward and toward the right wall.

3.3 Behaviors of Circulatory Cells Differ in Membrane Stiffness

In DPD formulation, the shear modulus μ_0 characterizes the stiffness of the cell's membrane. Thus, we increased the shear modulus from the range of RBC ($10^1\ pN/\mu m$) to 2 orders of magnitude greater range ($10^3\ pN/\mu m$). As previously discussed, a larger number of DPD particles are needed to accurately model the membrane dynamics in RBC's range. This explains the 660-particle configurations in the setup.

The behavior of circulatory cells in relation to their membrane stiffness has been studied in detail, as evidenced by the results presented in Figure 5. It was found that the spherical cell with the red blood cell (RBC) membrane's stiffness behaved similarly to this type of circulatory cell. The cell membrane deformed quickly and attained an equilibrium shape, which propagated along the flow in a straight line, with no visible rolling during maneuver.

However, when the membrane stiffness doubled within the first order of magnitude, the cell's trajectory became more chaotic and sensitive to instantaneous changes in the flow. Observing the tracers' paths, it was noted that the trajectory had multiple sudden changes, but no visible rolling occurred during the cell's maneuver. This was the case where the cell executed the quickest displacement toward the right wall.

From the latter half of the second order of magnitude to the white blood cell (WBC) range, rolling became a stable behavior. As depicted in Figure 5, the cases of 750 $pN/\mu m$ and 5000 $pN/\mu m$ had almost identical trajectories despite a significant leap in membrane stiffness value. These findings shed light on the behavior of circulatory cells in different membrane stiffness conditions and can inform future research in the field.

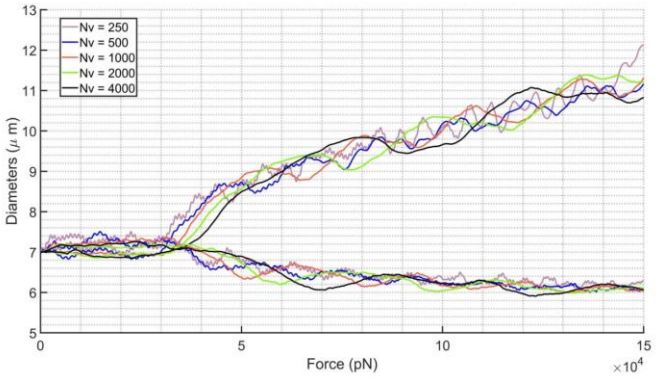

FIGURE 2. *THE EVOLUTION OF THE AXIAL AND TRANSVERSE DIAMETERS OF THE WBC VERSUS STRETCHING FORCE WHERE THE NUMBER OF DPD PARTICLES REPRESENTING THE MEMBRANE DIFFERS.*

Downloaded from http://asmedigitalcollection.asme.org/BIOMED/proceedings-pdf/DMD2024/87752/V001T02A009/7379084/v001t02a009-dmd2024-1076.pdf by guest on 28 January 2025

© 2024 by ASME

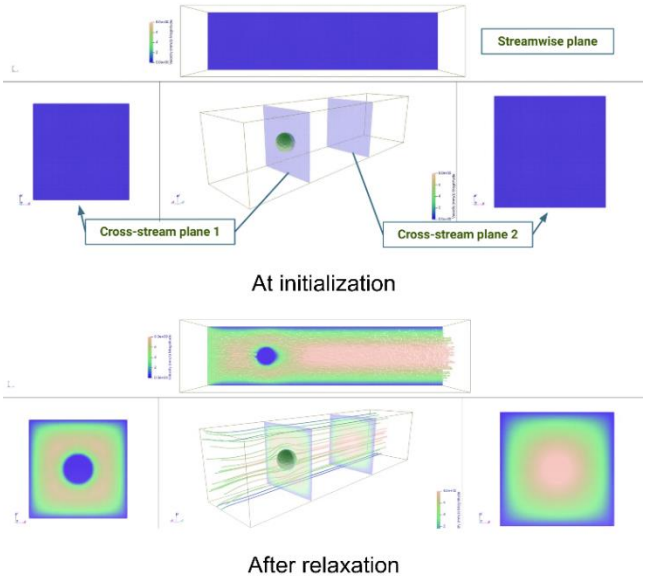

FIGURE 3. *STEADY-STATE SOLUTION OF THE NUMERICAL VELOCITY FIELD BY 3D INCOMPRESSIBLE NAVIER-STOKES SOLVER.*

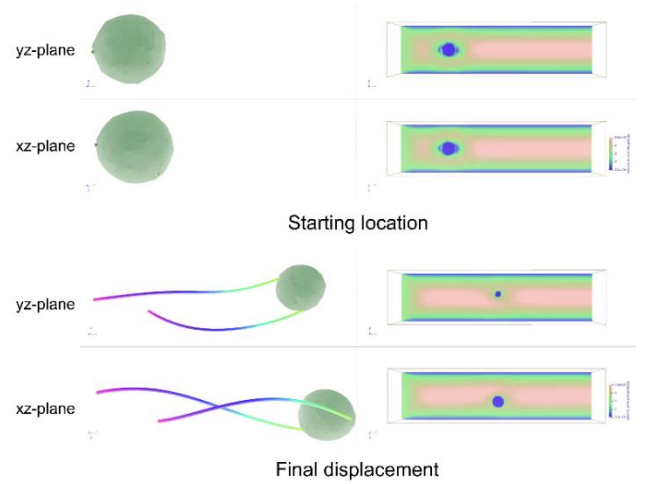

FIGURE 4. *TRAJECTORIES FROM TWO POINTS ON THE MEMBRANE SHOW THE WBC (IN GREEN) ROLLING BY INTERACTIONS WITH THE MICROCHANNEL FLOW.*

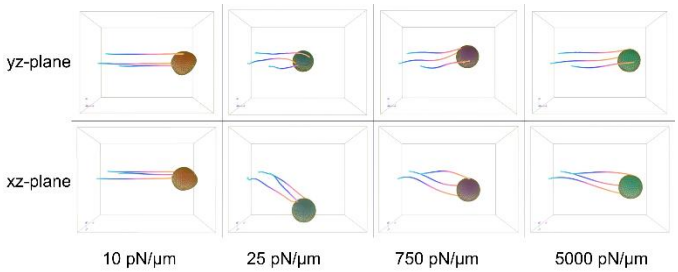

FIGURE 5. *DIFFERENT BEHAVIORS OF CIRCULATORY CELLS WHERE MEMBRANE STIFFNESS DIFFERS.*

4. CONCLUSION

In this work, we set up a numerical experiment to study how the membrane stiffness of a circulatory cell influences its dynamics in microchannel flows. The novel modeling approach of coupling the continuum method with the particle method performs fast and accurately for the cell's deformation under a low Reynolds number, pressure-driven flows (blood plasma). We successfully replicated the rolling dynamics of WBCs in the microchannel, which leads to the first conclusion that the rigid property of WBCs' membrane plays an important role in the margination process. Further tests showed three distinct patterns of cell-fluid interaction when membrane stiffness was varied by 2 orders of magnitude. In the future, the range of behaviors observed can be validated by applying correct experimental techniques to harden the RBC's membrane, i.e. RBCs in sickle cell anemia patients.

ACKNOWLEDGEMENTS

We acknowledge the financial support from the ND-EPSCoR via the ND-ACES grant (NSF #1946202). Our computational simulations in this study were performed using the computational resources of the Center for Computationally Assisted Science and Technology (CCAST) at North Dakota State University. We want to express our deepest gratitude toward Dr. Amit Joshi of the Medical College of Wisconsin for providing us with an excellent experiment movie and professional insights that led us to the subject of this study.

REFERENCES

[1] Secomb, Timothy W. Blood Flow in the Microcirculation. *Annu. Rev. Fluid Mech*. **2017**; 49: 443-461

[2] Fedosov, D.A., Caswell, B., Popell, A.S. and Karniadakis, G.E. Blood Flow and Cell-Free Layer in Microvessels. *Microcirculation*. **2010**; 17: 615-628

[3] Fedosov, Dmitry A. and Fornleitner, Julia and Gompper, Gerhard. Margination of White Blood Cells in Microcapillary Flow. *Phys. Rev. Lett*. **2012**; 108(2): 028104

[4] N. Takeishi, Y. Imai, K. Nakaaki, T. Yamaguchi, T. Ishikawa. Leukocyte margination at arteriole shear rate. *Physiol Rep*. **2014**; 2(6): e12037

[5] Qi, X., Wang, W., Ma, S., Han, K., Bian X., Li X. Quantitative prediction of rolling dynamics of leukocyte-inspired microroller in blood flow. *Physics of Fluids*. **2021**; 33 (12): 121908

[6] Akerkouch L, Le TB. A Hybrid Continuum-Particle Approach for Fluid-Structure Interaction Simulation of Red Blood Cells in Fluid Flows. *Fluids*. **2021**; 6(4):139

[7] Le, T.B.; Borazjani, I.; Sotiropoulos, F. Pulsatile flow effects on the hemodynamics of intracranial aneurysms. *J. Biomech. Eng.* **2010**; 132:1-11

Downloaded from http://asmedigitalcollection.asme.org/BIOMED/proceedings-pdf/DMD2024/87752/V001T02A009/7379084/v001t02a009-dmd2024-1076.pdf by guest on 28 January 2025

© 2024 by ASME